



Nucleation and early stages of growth of lead onto copper electrodes from dilute electrolytes

Nebojša D. NIKOLIĆ¹, Sanja I. STEVANOVIĆ¹, Goran BRANKOVIĆ²

1. ICTM–Department of Electrochemistry, University of Belgrade, Njegoševa 12, Belgrade, Serbia;
2. Institute for Multidisciplinary Research, University of Belgrade, Kneza Višeslava 1a, Belgrade, Serbia

Received 25 December 2015; accepted 11 April 2016

Abstract: The processes of nucleation and growth of lead from the dilute electrolytes on copper substrates were investigated by chronoamperometry and by scanning electron microscopic (SEM) analysis of the deposits obtained in the potentiostatic regime of electrolysis. In the dependence of electrodeposition conditions, the nucleation of Pb followed either progressive or instantaneous type. The type of nucleation changed from progressive to instantaneous one with increasing the concentration of Pb(II) ions and the overpotential of electrodeposition. Regardless of the type nucleation, a novel type of Pb particles like cobweb was formed by the potentiostatic electrodeposition in the moment of nucleation and at the early stages of growth. On the basis of the shape of cobweb-like particles and the electrodeposition conditions leading to their formation, these particles were situated in the group of spongy-like ones. Also, comparative morphological analysis of Pb deposits obtained in the conditions of progressive and instantaneous nucleation confirmed the existence of two limiting types of nucleation.

Key words: electrodeposition; lead; nucleation; growth; morphology; chronoamperometry

1 Introduction

Electrodeposition technique is very promising way to obtain metal at the micro or nano scale in the form suitable for application in various technologies. The desired morphology of electrodeposited pure metals or alloys is attained by the choice of regime and by easy control of parameters of electrolysis, such as current density or overpotential of electrodeposition, temperature of electrolysis, solution composition, type of working electrode, time of electrolysis, addition of additives [1–4]. Simultaneously, the morphology of metal deposits strongly depends on the nature of metals, and metals are usually classified in the dependence of values of the exchange current density and overpotential for hydrogen discharge on normal, intermediate and inert ones [5]. The similar effects of parameters of electrolysis on the surface morphology were observed during electrolysis from both the aqueous electrolytes and ionic liquids [6–8].

Lead (Pb) is the typical representative of normal metals which attracts both academic and technological attention thanks to its specific characteristics, such as

extremely high reactivity and superconductivity [9]. Due to these characteristics, Pb has found wide application as high purity active material for acid batteries [10], semiconductors [11,12] and in the fabrication of electrochromic devices [13]. The processes of Pb electrodeposition belong to the fast electrochemical processes because they are characterized by the extremely high exchange current density and high hydrogen overpotential discharge values. The main characteristics of these processes are fast charge-transfer step, formation of irregular deposits starting from relatively small overpotentials and the absence of obtaining of compact deposits without use of additives [1]. The electrolysis from the aqueous electrolytes is the most often used way to obtain Pb in the form suitable for some of above mentioned applications. The different electrolytes including both acid [14–18] and alkaline [19–21] ones are widely used for the processes of Pb electrodeposition. In the last time, electrolysis from choline chloride–urea deep eutectic solvents is also used to obtain Pb in the desired form [22,23].

In the dependence of conditions of electrolysis, Pb electrodeposition processes from aqueous electrolytes lead to the formation of both isotropic and anisotropic

morphological forms, such as octahedrons, hexagons, twinned particles, wires, needle-like and honeycomb-like structures, as well as two-dimensional (2D) dendrites of different shapes (fern-like and tooth of saw ones) [9,15,16,24–29]. There was no any difference in Pb surface morphologies obtained by electrolysis from aqueous electrolytes and those obtained from deep eutectic solvents [22,23].

Chronoamperometry is widely often way to analyze the processes of nucleation and the early stages of growth. SCHARIFKER et al [30–32] developed the theoretical model enabling to determine the type of nucleation by comparison of the experimental data obtained by the analysis of the potentiostatic current transients with their model. The model proposed by SCHARIFKER et al [30–32] was based on the three-dimensional (3D) nucleation with diffusion-controlled growth and they predicted two limiting cases for nucleation processes: progressive and instantaneous. In the instantaneous nucleation, all nuclei are formed simultaneously at the very beginning of electrodeposition process, while in the progressive nucleation type the number of nuclei increases with time prolonging. This model is widely used for the analysis of nucleation/growth processes from both aqueous electrolytes [33–36] and deep eutectic solvents [37,38]. However, in these investigations, little attention is devoted to morphological analysis of deposits formed in the early stages of metal growth without clear correlation between the type of nucleation and the surface morphology. Considering the fact that the morphology is the most important characteristic of electrodeposited metal, in this study, we correlate the limiting types of nucleation with morphology of lead deposits formed in the moment of nucleation and at the early stages of growth.

2 Experimental

Lead was electrodeposited at the overpotentials of 25, 37.5, 50 and 62.5 mV from the following electrolytes: (a) 0.010 mol/L $\text{Pb}(\text{NO}_3)_2$ in 2.0 mol/L NaNO_3 , (b) 0.030 mol/L $\text{Pb}(\text{NO}_3)_2$ in 2.0 mol/L NaNO_3 , and (c) 0.045 mol/L $\text{Pb}(\text{NO}_3)_2$ in 2.0 mol/L NaNO_3 .

All electrodepositions were performed in open cell at room temperature, using Autolab potentiostat/galvanostat PGStat 128N (ECO Chemie, The Netherlands). Electrodeposition of lead was performed on the cylindrical copper electrodes. The surface area of Cu electrodes was 0.25 cm². The reference and counter electrodes were of pure lead. The counter electrode was a lead foil with a surface area of 0.80 dm² that was placed close to the cell walls. The reference electrode was a lead wire of which the tips were positioned at a distance of

about 0.2 cm from the surface of the working electrodes. The working electrodes were placed in the centre of cell, at the same location for each experiment. Doubly distilled water and analytical grade chemicals were used for the preparation of electrolytes for Pb electrodeposition.

Lead deposits electrodeposited from 0.010 mol/L $\text{Pb}(\text{NO}_3)_2$ in 2.0 mol/L NaNO_3 at overpotentials of 25 and 62.5 mV were characterized using a scanning electron microscope (SEM)–TESCAN Digital Microscope.

3 Results and discussion

3.1 Nucleation and kinetics of Pb electrodeposition processes

Figure 1 represents the potentiostatic current transients obtained in the Pb electrodeposition processes at overpotentials of 25, 37.5, 50 and 62.5 mV from 0.010, 0.030 and 0.045 mol/L $\text{Pb}(\text{NO}_3)_2$ in 2.0 mol/L NaNO_3 electrolytes. All shown the potentiostatic current transients represent the typical diffusion controlled ones characterized by the increase in the current density up to maximum and the sharp decrease until the limiting diffusion current density was reached. The increase in the current density corresponds to the process of nucleation and to the growth of existing nucleus, while the descending part corresponds to the linear diffusion to the planar electrode surface. From Fig. 1, it can be noticed that the decrease in the time corresponding to the maximum current density was observed with increasing the overpotential of electrodeposition.

The shape of the potentiostatic current transients clearly indicates that it is possible to apply a model proposed by SCHARIFKER et al [30–32] to determine the type of nucleation. For the determination of type of nucleation, the dimensionless dependencies $(J/J_m)^2 - t/t_m$ were derived from the potentiostatic current transients and compared with the theoretical predictions for instantaneous:

$$\left(\frac{J}{J_m}\right)^2 = \frac{1.9542}{(t/t_m)} \left\{ 1 - \exp \left[-1.2564 \left(\frac{t}{t_m}\right) \right] \right\}^2 \quad (1)$$

and progressive:

$$\left(\frac{J}{J_m}\right)^2 = \frac{1.2254}{(t/t_m)} \left\{ 1 - \exp \left[-2.3367 \left(\frac{t}{t_m}\right)^2 \right] \right\}^2 \quad (2)$$

nucleation and growth [30–32]. In this way, the dependencies shown in Fig. 2 are obtained from the potentiostatic current transients shown in Fig. 1.

In Eqs. (1) and (2), a time t_m corresponds to the maximum of current density (J_m) in the potentiostatic current transients. It can be seen from Fig. 2 that

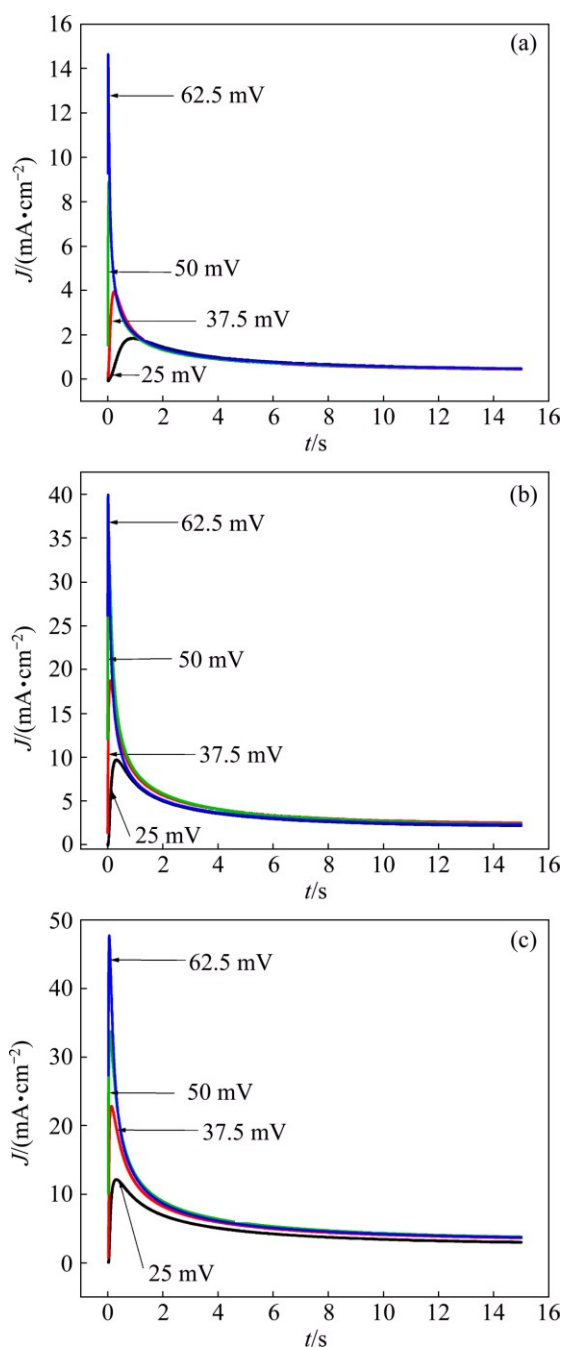


Fig. 1 Potentiostatic current transients obtained in lead electrodeposition process at overpotentials of 25, 37.5, 50 and 62.5 mV from 0.010 (a), 0.030 (b), 0.045 (c) mol/L $\text{Pb}(\text{NO}_3)_2$ in 2.0 mol/L NaNO_3 electrolytes

nucleation changes from progressive to instantaneous type with increasing the concentration of $\text{Pb}(\text{II})$ ions and with increasing the overpotential of the electrodeposition. The progressive type of nucleation corresponds to electrodeposition process from the electrolyte containing 0.010 mol/L Pb^{2+} ions at overpotentials of 25 and 37.5 mV, and the transition towards the instantaneous type is observed with increasing the overpotential of electrodeposition, reaching this nucleation type already at 62.5 mV. On the other hand, the increasing

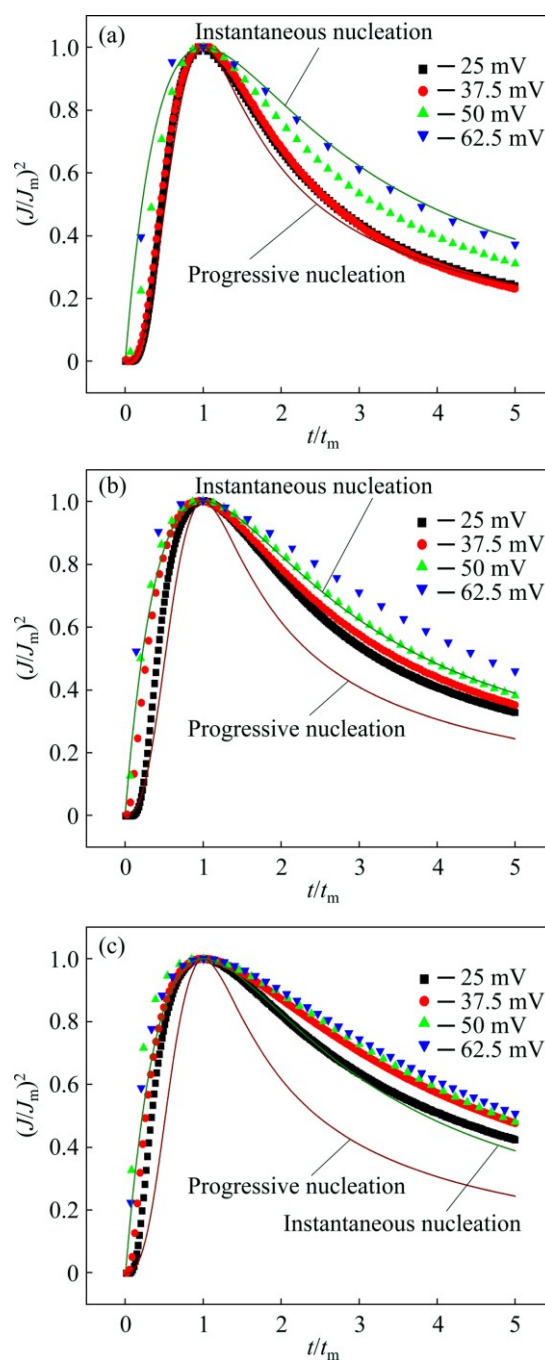


Fig. 2 Dimensionless dependencies $(J/J_m)^2 - t/t_m$ derived from potentiostatic current transients shown in Fig. 1: (a) 0.010, (b) 0.030, (c) 0.045 mol/L $\text{Pb}(\text{NO}_3)_2$ in 2.0 mol/L NaNO_3

concentration of $\text{Pb}(\text{II})$ ions causes the decrease of the overpotential at which the instantaneous type of nucleation is attained (0.030 mol/L Pb^{2+} , $\eta=50$ mV, Fig. 2(b); and 0.045 mol/L Pb^{2+} , $\eta=25$ mV, Fig. 2(c)). Above these overpotentials, the deviation from the theoretical prediction for the instantaneous nucleation type is observed, which can be ascribed to the fast change of the real electrode surface caused by the high current density of electrodeposition in the early stages of electrodeposition.

The diffusion coefficients are calculated from the descending parts of the potentiostatic current transients by application of Cottrell equation [37]:

$$J = nFc(D/\pi)^{1/2}t^{-1/2} \quad (3)$$

where nF is the molar charge transferred during electrodeposition, c is the bulk concentration of the electroactive species, D is the diffusion coefficient, and t is time. The values of decreasing current densities after the current maximum were plotted with $t^{-1/2}$, and the obtained dependencies for the examined electrolytes are presented in Fig. 3. The values of the diffusion coefficients obtained in this way were summarized in Table 1. As expected, the diffusion coefficients do not depend on the overpotential of the electrodeposition. From Table 1, it can be concluded that the values of diffusion coefficients are in excellent agreement with those found by MOSTANY et al [32] for this type of electrolyte. The slight deviation in the value of diffusion coefficient observed at 25 mV from the electrolyte containing 0.030 mol/L Pb^{2+} , and the small segment at the ordinate observed at the same overpotential from 0.045 mol/L Pb^{2+} (see insert in Fig. 3(c)) can be ascribed to the traces of ohmic control in Pb electrodeposition processes at very low overpotentials. Namely, in the electrolytes with higher concentrations of Pb^{2+} ions, the electrodeposition process is the ohmic controlled at the low overpotentials, and the ratio of the ohmic control to the overall control of electrodeposition increases with increasing concentration of Pb^{2+} ions [15,39].

3.2 SEM study

The maximum current density in the potentiostatic current transients and the early stages of growth was characterized by the analysis of Pb deposits obtained under the conditions of progressive and instantaneous nucleation using SEM technique. Figures 4 and 5 show Pb deposits produced from 0.010 mol/L $Pb(NO_3)_2$ in 2.0 mol/L $NaNO_3$ at overpotentials of 25 mV (the progressive nucleation, Fig. 4) and 62.5 mV (the instantaneous nucleation, Fig. 5). In both cases, the time of electrodeposition corresponding to $t/t_m=1$, $t/t_m=5$ and $t/t_m=50$ were analyzed. From Figs. 4 and 5, it can be noticed that the 3D cobweb-like particles were formed in the both cases. This form of Pb particles has been completely different from all morphological forms of lead observed so far [9,15,16,24–29], indicating that it represents novel type of Pb surface morphology. On the basis of analysis of the shape of cobweb-like particles, it can be concluded that these particles belong to the group of spongy-like deposits [1,40,41].

The spongy-like particles have been already observed during the electrodeposition of cadmium and zinc, and for the first time, they were observed during Pb

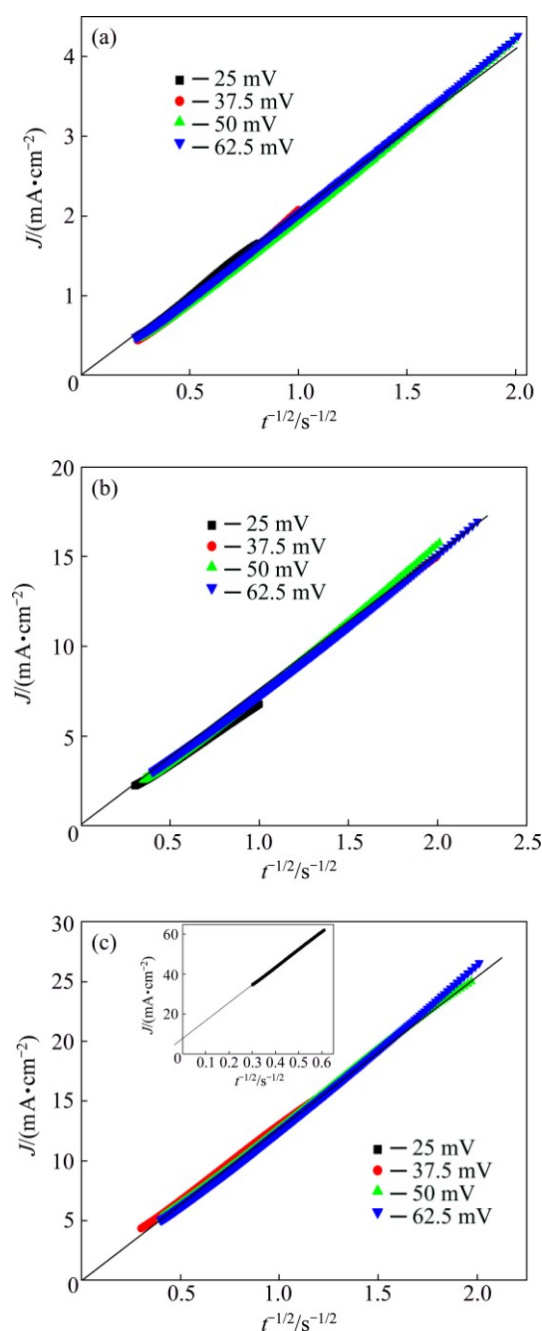


Fig. 3 Determination of diffusion coefficients by application of Cottrell equation: (a) 0.010; (b) 0.030; (c) 0.045 mol/L $Pb(NO_3)_2$ in 2.0 mol/L $NaNO_3$

Table 1 Values of diffusion coefficients calculated from Cottrell equation for electrolytes of different concentrations of Pb(II) ions (in 2.0 mol/L $NaNO_3$)

| η/mV | $D/(10^{-5}cm^2 \cdot s^{-1})$ | | |
|-----------|--------------------------------|-----------------------|-----------------------|
| | 0.010 mol/L Pb^{2+} | 0.030 mol/L Pb^{2+} | 0.045 mol/L Pb^{2+} |
| 25 | 0.335 | 0.433 | – |
| 37.5 | 0.330 | 0.515 | 0.687 |
| 50 | 0.344 | 0.517 | 0.676 |
| 62.5 | 0.349 | 0.513 | 0.670 |

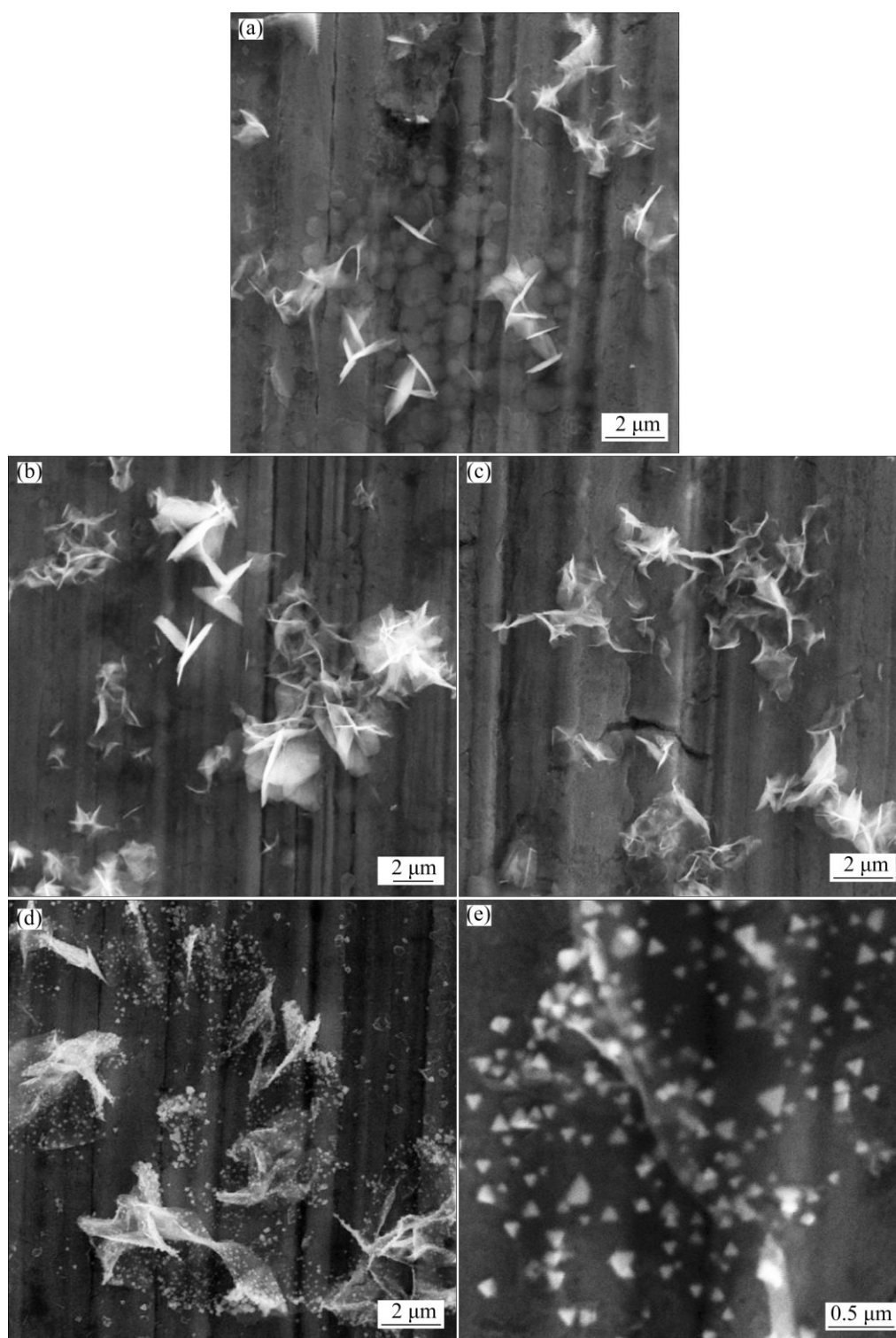


Fig. 4 Morphologies of Pb particles obtained by electrodeposition from 0.010 mol/L $\text{Pb}(\text{NO}_3)_2$ in 2.0 mol/L NaNO_3 electrolyte at overpotential of 25 mV (progressive nucleation): (a) $t/t_m=1$ ($t=0.9175$ s); (b, c) $t/t_m=5$ ($t=4.5875$ s); (d, e) $t/t_m=50$ ($t=45.875$ s)

electrodeposition in this investigation. The common feature of Pb, Cd and Zn is affiliation to the same group of metals, i.e., to the group of normal metals (the high exchange current density; the high overpotential for hydrogen evolution reaction [5]). Aside from the shape of cobweb-like particles, the other features determining

the spongy-like growth, such as formation at the low overpotentials and low nucleation density of the formed nuclei, were also fulfilled. In the case of Pb, the low nucleation density is attained by very small current density of electrodeposition caused by the use of very dilute electrolytes.

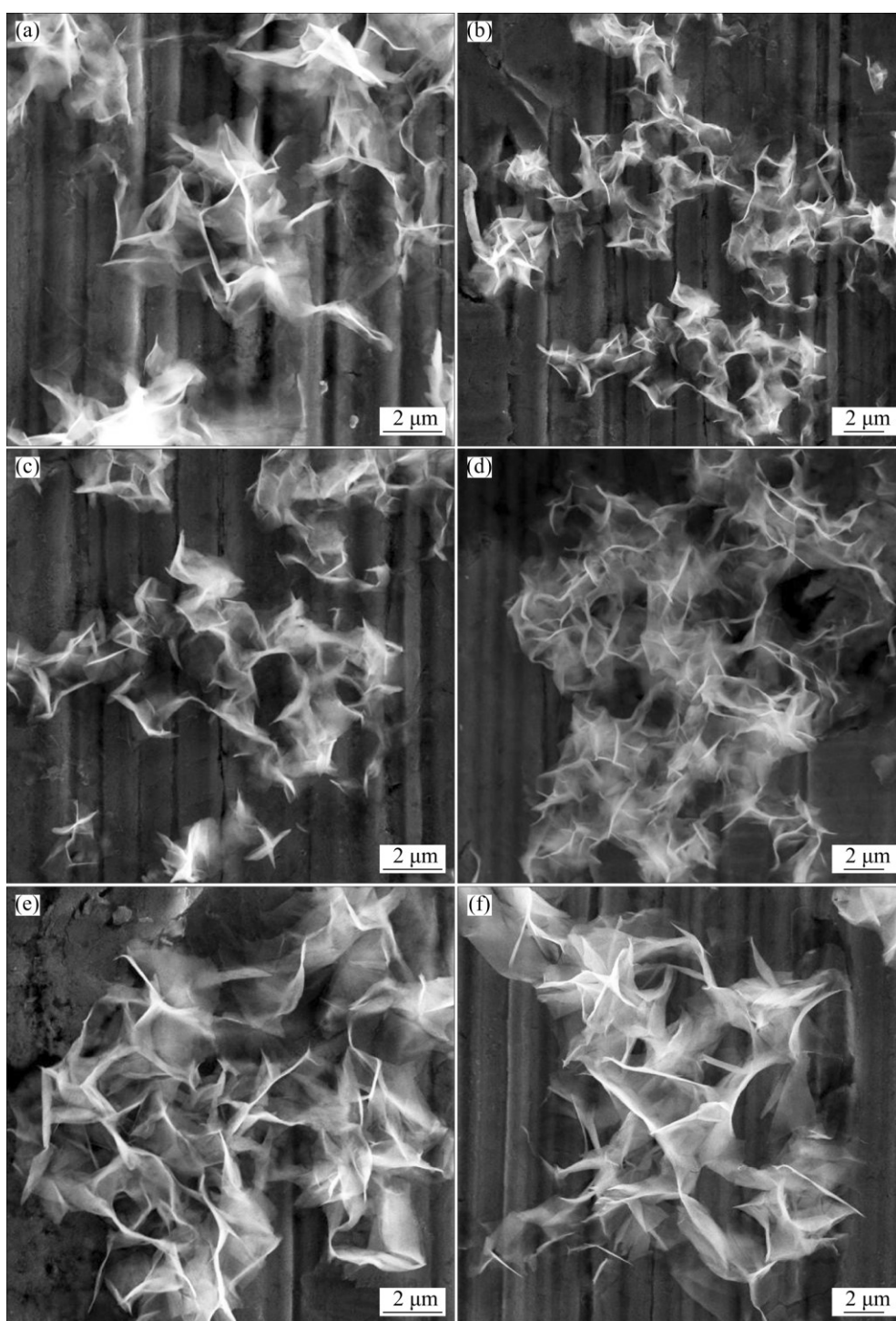


Fig. 5 Morphologies of Pb particles obtained by electrodeposition from 0.010 mol/L $\text{Pb}(\text{NO}_3)_2$ in 2.0 mol/L NaNO_3 electrolyte at overpotential of 62.5 mV (instantaneous nucleation): (a) $t/t_m=1$ ($t=0.0125$ s); (b, c) $t/t_m=5$ ($t=0.0625$ s); (d, e) $t/t_m=50$ ($t=0.625$ s); (f) $t=45.875$ s

Then, the theory of formation of the spongy deposits can be applied and considered as follows: the formation of a spongy deposit is caused by mass-transport limitations when the nucleation rate is low, and for the systems where $J_L < J_0$ like Pb, the condition for the formation of spongy-like particles is fulfilled at low overpotentials.

At low overpotential a small number of nuclei are formed, and they can grow independently. The spherical diffusion layer is formed around each independently formed nucleus, and the limiting diffusion current density to the growing nucleus, $J_{L,N}$ (or the limiting current density under spherical diffusion control) is given by Eq. (4) [1]:

$$J_{L,N} = \frac{nFDc}{r_N} \quad (4)$$

or

$$J_{L,N} = \frac{j_L \delta}{r_N} \quad (5)$$

Since

$$J_L = \frac{nFDc}{\delta} \quad (6)$$

where r_N is the tip radius of the nucleus, δ is the diffusion layer thickness, J_L is the limiting diffusion current density for steady-state linear diffusion.

The spongy growth is initiated by the amplification of surface protrusions directly inside the spherical diffusion layer formed around each independently growing nucleus. The growth of protrusions in all directions is good proof that the initial stage of deposition on the nuclei is under spherical diffusion control, while further growth occurs in the diffusion layer of the macroelectrode. With increasing the electrodeposition time, the protrusions branch and interweave making cobweb-like character of the formed particles.

From the above presented results, it can be concluded that the processes of Pb electrodeposition really follow the model proposed by SCHARIFKER et al [30–32] based on the 3D nucleation with diffusion controlled growth. This model is originally proposed for the diffusion controlled growth of hemispherical particles around which the spherical diffusion layer is formed. Anyway, it is clear that this model can be applied when many other irregular forms, such as needle-like in the case of bismuth [34], dendritic ones in the case of copper [37], or cobweb-like in the case of Pb (shown here), are formed in the growth process. The common characteristic of these irregular (or disperse) forms is the formation of spherical diffusion layer around the tips of surface protrusions of which they are formed.

Also, for the first time in this investigation the difference between the progressive and instantaneous nucleation was experimentally proved by morphological analysis. The increase in number of nuclei with the time, as well as the difference in their size, is clearly seen in the progressive type of nucleation (Fig. 4). In the moment of nucleation, small number of the cobweb-like particles are formed (Fig. 4(a)). The difference in their size observed after $t/t_m=5$ clearly indicates that the smaller particles are formed later (the progressive formation of particles, Figs. 4(b) and (c)). With the further prolongation of electrodeposition time ($t/t_m=50$, Figs. 4(d) and (e)), the number of nuclei increases strongly and the large number of regular particles like

octahedrons of nano size dimensions are formed among large cobweb-particles (Fig. 4(e)). Simultaneously, the new nucleation is not observed in the case of instantaneous nucleation, but only growth and coalescence of neighboring cobweb-like particles (Figs. 5(a)–(e)). Furthermore, the new nucleation is not observed and for the longer electrodeposition time ($t=45.875$ s, Fig. 5(f)), i.e., in the time which corresponded to $t/t_m=50$ in the progressive type of nucleation (Figs. 4(d) and (e)).

Formation of nano size cobweb-particles can be primarily correlated with a concentration of Pb^{2+} ions. Namely, this type of particles is only formed from the dilute electrolytes, and it is not strictly associated with the overpotential of electrodeposition. In the case of concentrated electrolytes, various disperse forms, such as regular hexagonal particles, irregular crystals (precursors of dendrites) and dendrites of different shape, are formed at the overpotentials corresponding to the formation of the spongy-like particles in the dilute electrolytes.

4 Conclusions

Correlation between the processes of nucleation/growth and morphology of Pb deposits obtained in the moment of nucleation and at the early stage of electrodeposition process was made. The novel type of Pb particles similar to cobweb-one was detected during electrodeposition from the dilute electrolytes under the conditions of both the progressive and instantaneous nucleation. On the basis of the shape and parameters leading to their formation, these particles are classified in the group of spongy-like one. For the first time, the nucleation/growth phenomena under the conditions of progressive and instantaneous nucleation were examined at the same time by SEM technique and the difference between these two types of nucleation was proved through morphological analysis of formed deposits.

Acknowledgement

This work was supported by the Ministry of Education, Science and Technological Development of the Republic of Serbia under the research project: “Electrochemical synthesis and characterization of nanostructured functional materials for application in new technologies” (Project No. 172046).

References

- [1] POPOV K I, DJOKIĆ S S, GRGUR B N. Fundamental aspects of electrometallurgy [M]. New York: Kluwer Academic/Plenum Publishers, 2002: 78–89.
- [2] PATNAIK P, PADHY S K, TRIPATHY B C, BHATTACHARYA I N, PARAMGURU R K. Electrodeposition of cobalt from aqueous sulphate solutions in the presence of tetra ethyl ammonium

- bromide [J]. Transactions of Nonferrous Metals Society of China, 2015, 25: 2047–2053.
- [3] ZAMANI M, AMADEH A, LARI BAGHAL S M. Effect of Co content on electrodeposition mechanism and mechanical properties of electrodeposited Ni–Co alloy [J]. Transactions of Nonferrous Metals Society of China, 2016, 26: 484–491.
- [4] CAO Hua-zhen, ZHONG Yang, WU Lian-kui, ZHANG Yu-feng, ZHENG Guo-qu. Electrodeposition of As–Sb alloy from high arsenic-containing solutions [J]. Transactions of Nonferrous Metals Society of China, 2016, 26: 310–318.
- [5] WINAND R. Electrodeposition of metals and alloys—New results and perspectives [J]. *Electrochimica Acta*, 1994, 39: 1091–1105.
- [6] GONG Kai, HUA Yi-xin, XU Cun-ying, ZHANG Qi-bo, LI Yan, RU Juan-jian, JIE Ya-fei. Electrodeposition behavior of bright nickel in air and water-stable betaine-HCl–ethylene glycol ionic liquid [J]. Transactions of Nonferrous Metals Society of China, 2015, 25: 2458–2465.
- [7] QIAN Jian-gang, YIN Ying, LI Xin, LI Tie-jun. Electrodeposition of iridium from composite ionic liquid [J]. Transactions of Nonferrous Metals Society of China, 2015, 25: 1685–1691.
- [8] FASHU S, GU Chang-dong, ZHANG Jia-lei, HUANG Mei-ling, WANG Xiu-li, TU Jiang-ping. Effect of EDTA and NH_4Cl additives on electrodeposition of Zn–Ni films from choline chloride-based ionic liquid [J]. Transactions of Nonferrous Metals Society of China, 2015, 25: 2054–2064.
- [9] YAO Chen-zhong, LIU Meng, ZHANG Peng, HE Xiao-hui, LI Gao-ren, ZHAO Wen-xia, LIU Peng, TONG Ye-xiang. Tuning the architectures of lead deposits on metal substrates by electrodeposition [J]. *Electrochimica Acta*, 2008, 54: 247–253.
- [10] PAVLOV D. Premature capacity loss (PCL) of the positive lead/acid battery plate: A new concept to describe the phenomenon [J]. *Journal of Power Sources*, 1993, 42: 345–363.
- [11] RASHKOVA B, GUEL B, POTZSCHKE R T, STAIKOV G, LORENZ W J. Electrodeposition of Pb on n-Si(111) [J]. *Electrochimica Acta*, 1998, 43: 3021–3028.
- [12] EHLERS C, KONIG U, STAIKOV G, SCHULTZE J W. Role of surface states in electrodeposition of Pb on n-Ge(111) [J]. *Electrochimica Acta*, 2002, 47: 379–385.
- [13] AVELLANEDA C O, NAPOLITANO M A, KAIBARA E K, BULHOES L O S. Electrodeposition of lead on ITO electrode: Influence of copper as an additive [J]. *Electrochimica Acta*, 2005, 50: 1317–1321.
- [14] NIKOLIĆ N D, BRANKOVIĆ G, LAČNJEVAC U Č. Formation of two-dimensional (2D) lead dendrites by application of different regimes of electrolysis [J]. *Journal of Solid State Electrochemistry*, 2012, 16: 2121–2126.
- [15] NIKOLIĆ N D, POPOV K I, ŽIVKOVIĆ P M, BRANKOVIĆ G. A new insight into the mechanism of lead electrodeposition: Ohmic–diffusion control of the electrodeposition process [J]. *Journal of Electroanalytical Chemistry*, 2013, 691: 66–76.
- [16] NIKOLIĆ N D, VAŠTAG Dj Dj, ŽIVKOVIĆ P M, JOKIĆ B, BRANKOVIĆ G. Influence of the complex formation on the morphology of lead powder particles produced by the electrodeposition processes [J]. *Advanced Powder Technology*, 2013, 24: 674–682.
- [17] MOSTANY J, PARRA J, SCHARIFKER B R. The nucleation of lead from halide-containing solutions [J]. *Journal of Applied Electrochemistry*, 1986, 16: 333–338.
- [18] PLETCHER D, WILLS R. A novel flow battery: A lead acid battery based on an electrolyte with soluble lead(II). Part II. Flow cell studies [J]. *Physical Chemistry Chemical Physics*, 2004, 6: 1779–1785.
- [19] WONG S M, ABRANTES L M. Lead electrodeposition from very alkaline media [J]. *Electrochimica Acta*, 2005, 51: 619–626.
- [20] GU Ying-ying, ZHOU Qiong-hua, YANG Tian-zu, LIU Wei, ZHANG Du-chao. Lead electrodeposition from alkaline solutions containing xylitol [J]. Transactions of Nonferrous Metals Society of China, 2011, 21: 1407–1413.
- [21] NIKOLIĆ N D, VAŠTAG Dj Dj, MAKSIMOVIĆ V M, BRANKOVIĆ G. Morphological and crystallographic characteristics of lead powder obtained by electrodeposition from an environmentally friendly electrolyte [J]. Transactions of Nonferrous Metals Society of China, 2014, 24: 884–892.
- [22] RU Juan-jian, HUA Yi-xin, XU Cun-ying, LI Jian, LI Yan, WANG Ding, QI Can-can, JIE Ya-fei. Morphology-controlled preparation of lead powders by electrodeposition from different PbO-containing choline chloride-urea deep eutectic solvent [J]. *Applied Surface Science*, 2015, 335: 153–159.
- [23] RU Juan-jian, HUA Yi-xin, XU Cun-ying, LI Jian, LI Yan, WANG Ding, GONG Kai, ZHOU Zhong-gren. Preparation of sub-micrometer lead wires from PbO by electrodeposition in choline chloride–urea deep eutectic solvent [J]. *Advanced Powder Technology*, 2015, 26: 91–97.
- [24] XIAO Z L, HAN C Y, KWOK W K, WANG H H, WELP U, WANG J, CRABTREE G W. Tuning the architecture of mesostructures by electrodeposition [J]. *Journal of the American Chemical Society*, 2004, 126: 2316–2317.
- [25] NI Yong-hong, ZHANG Yong-mei, HONG Jian-ming. Hierarchical Pb microstructures: A facile electrochemical synthesis, shape evolution and influencing factors [J]. *CrystEngComm*, 2011, 13: 934–940.
- [26] CHEREVKO S, XING Xiaoli, CHUNG Chan-Hwa. Hydrogen template assisted electrodeposition of sub-micrometer wires composing honeycomb-like porous Pb films [J]. *Applied Surface Science*, 2011, 257: 8054–8061.
- [27] NIKOLIĆ N D, MAKSIMOVIĆ V M, BRANKOVIĆ G. Morphological and crystallographic characteristics of electrodeposited lead from the concentrated electrolyte [J]. *RSC Advances*, 2013, 3: 7466–7471.
- [28] NIKOLIĆ N D, POPOV K I, IVANOVIĆ E R, BRANKOVIĆ G, STEVANOVIĆ S I, ŽIVKOVIĆ P M. The potentiostatic current transients and the role of local diffusion fields in formation of the 2D lead dendrites from the concentrated electrolyte [J]. *Journal of Electroanalytical Chemistry*, 2015, 739: 137–148.
- [29] NIKOLIĆ N D, IVANOVIĆ E R, BRANKOVIĆ G, LAČNJEVAC U Č, STEVANOVIĆ S I, STEVANOVIĆ J S, PAVLOVIĆ M G. Electrochemical and crystallographic aspects of lead granular growth [J]. *Metallurgical and Materials Transactions B*, 2015, 46: 1760–1774.
- [30] SCHARIFKER B, HILLS G. Theoretical and experimental studies of multiple nucleation [J]. *Electrochimica Acta*, 1983, 28: 879–889.
- [31] SCHARIFKER B, MOSTANY J. Three-dimensional nucleation with diffusion controlled growth. Part I. Number density of active sites and nucleation rates per site [J]. *Journal of Electroanalytical Chemistry*, 1984, 177: 13–23.
- [32] MOSTANY J, MOZOTA J, SCHARIFKER B. Three-dimensional nucleation with diffusion controlled growth. Part II. The nucleation of lead on vitreous carbon [J]. *Journal of Electroanalytical Chemistry*, 1984, 177: 25–37.
- [33] NASIRPOURI F. On the electrodeposition mechanism of Pb on copper substrate from a perchlorate solution studied by electrochemical quartz crystal microbalance [J]. *Ionics*, 2011, 17: 331–337.
- [34] YANG Minli, HU Zhongbo. Electrodeposition of bismuth onto glassy carbon electrodes from nitrate solutions [J]. *Journal of Electroanalytical Chemistry*, 2005, 583: 39–45.
- [35] WU Shi-xin, YIN Zong-you, HE Qi-yuan, LU Gang, YAN Qing-yu, ZHANG Hua. Nucleation mechanism of electrochemical deposition

- of Cu on reduced graphene oxide electrodes [J]. *Journal of Physical Chemistry C*, 2011, 115: 15973–15979.
- [36] USTARROZ J, KE X, HUBIN A, BALS S, TERRY H. New insights into the early stages of nanoparticle electrodeposition [J]. *Journal of Physical Chemistry C*, 2012, 116: 2322–2329.
- [37] ZHANG Q B, HUA Y X. Electrochemical synthesis of copper nanoparticles using cuprous oxide as a precursor in choline chloride–urea deep eutectic solvent: nucleation and growth mechanism [J]. *Physical Chemistry Chemical Physics*, 2014, 16: 27088–27095.
- [38] RU Juan-jian, HUA Yi-xin, XU Cun-ying, LI Jian, LI Yan, WANG Ding, QI Can-can, GONG Kai. Electrochemistry of Pb (II)/Pb during preparation of lead wires from PbO in choline chloride–urea deep eutectic solvent [J]. *Russian Journal of Electrochemistry*, 2015, 51: 773–781.
- [39] NIKOLIĆ N D, POPOV K I. A new approach to the understanding of the mechanism of lead electrodeposition [M]//DJOKIĆ S S. *Electrodeposition and Surface Finishing. Series: Modern Aspects of Electrochemistry*. Vol. 57. New York: Springer, 2014: 85–132.
- [40] POPOV K I, KRSTAJIĆ N V. The mechanism of spongy electrodeposits formation on inert substrate at low overpotentials [J]. *Journal of Applied Electrochemistry*, 1983, 13: 775–782.
- [41] POPOV K I, KRSTAJIĆ N V, ČEKEREVAČ M I. The mechanism of formation of coarse and disperse electrodeposits [M]//WHITE R E, CONWAY B E, BOCKRIS J O' M. *Modern Aspects of Electrochemistry*. Vol. 30. New York: Plenum Press, 1996: 261–312.

稀溶液中铅在铜电极上的成核和早期生长

Nebojša D. NIKOLIĆ¹, Sanja I. STEVANOVIĆ¹, Goran BRANKOVIĆ²

1. ICTM – Department of Electrochemistry, University of Belgrade, Njegoševa 12, Belgrade, Serbia;
2. Institute for Multidisciplinary Research, University of Belgrade, Kneza Višeslava 1a, Belgrade, Serbia

摘要: 采用计时电流方法和对恒电位电解得到的沉积产物进行 SEM 观察, 研究稀溶液中铅在铜电极上的成核和生长过程。根据电沉积条件不同, 铅的成核分为连续成核和瞬时成核两种形式。随着溶液中 Pb(II)浓度和电沉积时超电势的增加, 成核形式从连续成核转变为瞬时成核。无论是哪种成核形式, 在恒电位电解的成核和早期生长阶段, 生成的铅颗粒都是蛛网状的。根据蛛网状颗粒的形状和导致它们生成的电沉积条件, 这些颗粒属于海绵状颗粒。对连续成核和瞬时成核条件下的铅沉积产物的形貌观察表明, 存在两种成核极限。

关键词: 电沉积; 铅; 成核; 生长; 形貌; 计时电流法

(Edited by Sai-qian YUAN)